

12-2012

# Intracellular Expression of an Ice Nucleation Protein Reduces Cryoinjury in Insect Cells

Avril M. Harder  
*Eastern Illinois University*

Follow this and additional works at: <http://thekeep.eiu.edu/honors>



Part of the [Biology Commons](#)

---

## Recommended Citation

Harder, Avril M., "Intracellular Expression of an Ice Nucleation Protein Reduces Cryoinjury in Insect Cells" (2012). *Honors Theses*. 1.  
<http://thekeep.eiu.edu/honors/1>

This Article is brought to you for free and open access by the Student Theses & Publications at The Keep. It has been accepted for inclusion in Honors Theses by an authorized administrator of The Keep. For more information, please contact [tabruns@eiu.edu](mailto:tabruns@eiu.edu).

Intracellular Expression of an Ice Nucleation Protein Reduces Cryoinjury in Insect Cells

by

Avril M. Harder

**HONORS THESIS**

SUBMITTED IN PARTIAL FULFILLMENT OF THE REQUIREMENTS FOR THE DEGREE OF

**BACHELOR OF SCIENCE IN BIOLOGICAL SCIENCES WITH HONORS**

AT EASTERN ILLINOIS UNIVERSITY

CHARLESTON, ILLINOIS

December 2012

I hereby recommend that this Honors Thesis be accepted as fulfilling this part of the undergraduate degree cited above:

Michael A Menze \_\_\_\_\_  
Thesis Director Date

\_\_\_\_\_  
Honors Program Director Date

## ABSTRACT

Exposure of insect cells to subzero temperatures typically leads to cell membrane disruption and lethal intracellular ice formation. This study seeks to examine the cryoprotective value of transgenically expressing a bacterial ice nucleation protein (INP) in *Spodoptera frugiperda* (Sf-21) cells. The bacterium *Pseudomonas syringae* naturally produces a membrane-bound INP (inaZ), capable of structuring water and initiating ice formation at temperatures as high as -2 °C. I hypothesized that intracellular expression of a genetically altered form of inaZ (*Ps*INP) in Sf-21 cells will mediate highly regulated ice nucleation when cells are cooled to -80 °C in a slow, controlled manner. I also predicted that cells expressing *Ps*INP (Sf-21-*Ps*INP) will maintain cell membrane integrity in greater proportions than wildtype cells (Sf-21-WT). Following one freeze-thaw cycle, 60% of Sf-21-WT cell membranes remained intact, while 72% of Sf-21-*Ps*INP cells maintained membrane integrity. This difference is statistically significant, and indicates that *Ps*INP expression helps to prevent cryoinjury during freezing, and positively impacts cell viability following thawing.

## **ACKNOWLEDGMENTS**

I would like to express my deep gratitude to Dr. Michael Menze for his invaluable guidance and advice. He has provided me with a wonderful introduction to the world of cell physiology research, and will be forever grateful for the opportunity to conduct my undergraduate project in his lab. I would also like to thank our collaborator, Dr. Nilay Chakraborty, for his contributions and for providing me with an engineer's perspective on this study. Finally, I extend my appreciation to the EIU Biological Sciences faculty and to the Honors College, for supporting undergraduate research, and for providing a productive learning environment.

**TABLE OF CONTENTS**

**Title Page .....i**

**Abstract .....ii**

**Acknowledgments .....iii**

**Table of Contents .....iv**

**Introduction.....1**

**Materials and Methods.....6**

**Results .....10**

**Discussion .....14**

**Conclusions .....17**

**Literature Cited .....18**

## INTRODUCTION

Under certain conditions some bacteria synthesize specific proteins that serve as nucleation centers for ice crystals (Gurian-Sherman and Lindow, 1993). These microorganisms present ice nucleation proteins (INPs) on the cell surface and efficiently catalyze ice formation at temperatures as warm as -2 °C (Gurian-Sherman and Lindow, 1993). First identified and isolated by Wolber et al. (1986) the product of the highly repetitive gene sequence *inaZ*, expressed by the bacterium *Pseudomonas syringae*, is a membrane-bound protein (*PsINP*); this protein provides a molecular foundation for the structuring of water molecules. A virtually ubiquitous epiphytic pathogen, *P. syringae* induces frost damage in sensitive plant tissues at temperatures around -5 °C. Two main hypotheses about the functions of INPs have been postulated: a) to grant the bacterium access to nutrients in plant tissue and b) to provide a means of dispersal via the water cycle (Lindow et al., 1982; Morris et al., 2007, 2008). Furthermore, increasing proficiency of a particular strain at encouraging ice formation directly correlates to amplified virulence (Morris et al., 2010). Commercially important aspects include ski resorts' use of the protein, manufactured under the label SnoMax® (York International, Victor, NY) to initiate snow (ice) crystallization at warmer temperatures; *PsINP* has also been examined as a candidate for cloud seeding applications as a mechanism of drought relief (Battan, 1969; Morris et al., 2004).

The ability of *PsINP* to initiate ice nucleation at -2 °C seems unremarkable, as water is traditionally assumed to freeze at 0 °C. However, a sample of pure water may be supercooled to below -40 °C before homogeneous nucleation is observed (Li et al., 2011). Homogeneous nucleation refers to the formation of ice simply by the aggregation of only

water molecules. When an aqueous solution contains some foreign solutes about which water molecules may accumulate (an INP, for example), the potential for heterogeneous nucleation exists. Any ice ‘embryo,’ consisting of a foreign particle surrounded by water molecules, has a conditional critical mass. This value must be reached in order for ice crystal growth to continue; below this critical mass, the embryo will disintegrate. At this critical mass, two opposing forces are in equilibrium: (1) any mass increase correlates to an increase in free energy ( $\Delta G$ ) which energetically favors shrinkage of the ice crystal, versus (2) the reduction of the surface free energy ( $\Delta G_F$ ) which is decreased when the embryo grows and the volume to surface area ratio increases (Mazur, 2010). In its capacity as a heterogeneous nucleator, *PsINP* exceeds this critical mass on its own, bypassing the normal physical restraints applied to small ice embryos.

To date, the tertiary structure of an INP has yet to be determined, and therefore, the mechanism by which ice formation is induced is poorly understood. Fortunately, advances in protein sequencing and computational modeling techniques may be combined to shed light on the mechanism by which INPs function at the molecular level. A second class of proteins that impacts crystallization of water is comprised of antifreeze proteins (AFPs). AFPs were first discovered in Antarctic fish over 40 years ago and have been identified in several organisms inhabiting environments with persistent subzero temperatures including bacteria, fungi, algae, plants, and arthropods. The molecular mechanisms by which AFPs inhibit ice-formation have been well characterized (DeVries et al., 1969; Gilbert et al., 2004; Hoshino et al., 2003; Janech et al., 2006; Fei et al., 2008; Hawes et al., 2011). Based on their antithetical functions, INPs and AFPs were not expected to be highly similar. However, these two groups of proteins share a highly

conserved, repetitive TXT amino acid motif (threonine followed by any inward pointing amino acid, then another threonine residue) that has been shown to play a crucial role in conferring ice-binding ability (Graether et al., 2000). Threonyl oxygens of an AFP (from the beetle *Tenebrio molitor*) can mimic the structure of oxygens in an ice crystal lattice, encouraging the binding of water molecules (Liou et al., 2000; Fig. 1).

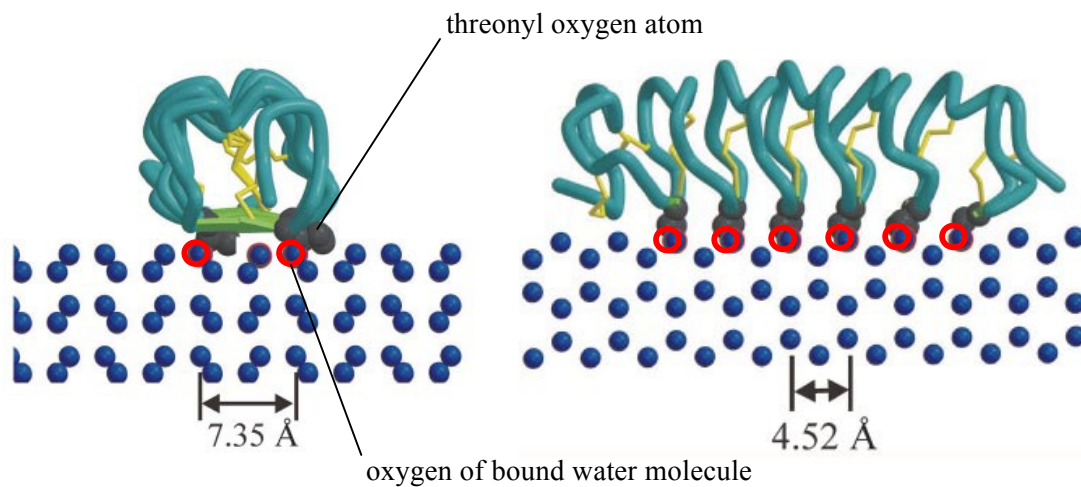


**Figure 1.** Association of threonyl oxygen atoms of an AFP in aqueous solution with oxygen atoms (outlined in red) of water molecules (adapted from Liou et al., 2000).

It is still poorly understood what specific properties of INPs and AFPs contribute to their dissimilar biological functions, given their similar associations with water molecules. Graether et al. (2001) suggested that the difference in the sheer mass of proteins might be responsible. INPs tend to be at least 10 times larger than AFPs, which could be a reflection of a minimum size requirement for an ice-forming surface with effective nucleation properties. Large INPs provide large surfaces that serve as a foundation for crystallization, whereas the binding sites of relatively smaller AFPs shield



ice nuclei from further aggregation (Graether et al., 2001). While this seems plausible, the exact mechanism of this phenomenon deserves further investigation.

Intracellular ice formation (IIF) is generally thought to be a lethal event, but the sources of cellular damage associated with IIF are uncertain. There are two popular hypotheses concerning the initiation of IIF: (1) extracellular ice simply propagates through preexisting pores in the cell membrane, initiating IIF, and (2) extracellular ice formation (EIF) is responsible for conformational changes in the structure of the cell membrane, rendering it an effective heterogeneous nucleator for intracellular ice (Mazur et al., 2005; Toner et al., 1993). Independent of the actual mechanism, EIF occurs prior to IIF. As the extracellular medium freezes, the concentration of solutes in the unfrozen portion increases, promoting osmotically-driven water flow from within the cell, and the maximum rate of this flow is set by the water permeability of the cell membrane (Mazur, 1963). This basic principle explains the impact of different cooling rates on cell membrane integrity during a freeze-thaw cycle. At slow cooling rates, intracellular water is able to flow out of the cell before IIF occurs, and at fast cooling rates, IIF is complete before any water traverses the cell membrane. Dumont et al. (2004) found that samples frozen at rates of  $5\text{ }^{\circ}\text{C} \cdot \text{min}^{-1}$  and  $30,000\text{ }^{\circ}\text{C} \cdot \text{min}^{-1}$  maintained higher proportions of cells with intact membranes than samples frozen at 180, 250, and  $5,000\text{ }^{\circ}\text{C} \cdot \text{min}^{-1}$ .

Additionally, studies conducted with the industrial product SnoMax® indicate that the protein, when present in extracellular medium, reduces the chaotic distribution of nucleation in solution and increases cell survival when present at sufficiently high concentrations (Missous et al., 2007). I hypothesized that intracellular expression of a water-structuring protein, such as *PsINP*, in combination with a slow, controlled cooling

rate ( $-1\text{ }^{\circ}\text{C} \cdot \text{min}^{-1}$ ) will allow for the orderly organization of water molecules during cell freezing, and membrane integrity will be maintained following thawing.

## MATERIALS AND METHODS

### **Sf-21 Cell Maintenance**

*Spodoptera frugiperda* (Sf-21) cells (Invitrogen Corporation, Carlsbad, CA) were cultured in 75 cm<sup>2</sup> cell culture flasks with Sf-900 III media (Invitrogen Corporation, Carlsbad, CA) at 26.5 °C. Penicillin (50 U/ml), streptomycin (50 g/ml), and amphotericin B (12.5 µg/ml) (MP Biomedicals, Solon, OH) were added to the Sf-900 III media. Cells were grown to a density of  $20 \cdot 10^6$  cells/flask and sub-cultured to  $1 \cdot 10^6$  cells per flask weekly.

### **Subcloning of the *Ps*INP gene**

A nucleotide sequence encoding for the central motif of INP from *Pseudomonas syringae* was synthesized (Gene Oracle, Mountain View, CA) and cloned into the pENTR/D-TOPO cloning vector (Invitrogen, Grand Islands, NY) following the protocol provided by the manufacturer. The *Ps*INP sequence was subcloned into the p1B/V-5-HIS-DEST vector for insect cell expression using clonase technology (Invitrogen, Grand Islands, NY).

### **Transfection of Sf-21 cells**

Three million Sf-21 cells were plated in 60 mm dishes at  $1.5 \cdot 10^6$  cells/ml in a total volume of 2 ml of Graces insect medium (Invitrogen Corporation, Carlsbad, CA). Cells were transfected using Lipofectamin according to the instructions of the supplier (Invitrogen Corporation, Carlsbad, CA). Stable insertion of the transgene was selected

for by exposing cells to 75 µg/ml of blasticidin for one month (Sf-21-*Ps*INP). After one month, cultures were maintained in 12.5 µg/ml blasticidin (MP Biomedicals, Solon, OH).

### **Buffer composition**

The buffer solution used in each of the following two assays was originally developed as a cell desiccation buffer, designed to increase tolerance of cells to water stress (buffer A). The buffer contains no conventional cryoprotective agents, but is comprised of: 40 ml 0.5 M potassium lactobionate solution per 250 ml buffer solution (35.83 g/200 ml H<sub>2</sub>O), MgCl • 6 H<sub>2</sub>O (3 mM), taurine (20 mM), HEPES (20 mM), KH<sub>2</sub>PO<sub>4</sub> (10 mM), bovine serum albumin (BSA, 0.25 g/250 ml), and trehalose (200 mM). The pH of the solution was adjusted to 6.8-7.0 with KOH.

### **Cell incubation assay**

Sf-21-*Ps*INP and Sf-21-WT cells were centrifuged at 3,000 • g for 5 min, washed with phosphate buffered saline (PBS), centrifuged again, and resuspended to a final density of approximately 1 • 10<sup>6</sup> cells/ml in buffer A. The cells were then incubated in a water bath at 27 °C for 4 h. A 20 µl sample was withdrawn each hour for cell membrane integrity assessment via trypan blue exclusion assay.

### **Freeze-thaw assay**

Cells were prepared in the same way as described above in buffer A. The resulting cell suspension was aliquoted in 1.0 ml samples into 2.0 ml cryovials (Fisher Scientific, Waltham, MA). Samples were frozen at a controlled rate of -1 °C • min<sup>-1</sup> using isopropanol in a Nalgene freezing container (Fisher Scientific, Waltham, MA).

Samples remained frozen for at least 24 h at -80 °C, and were rapidly thawed (< 120 sec) in a 27 °C water bath. Cell membrane integrity was immediately evaluated, again using the trypan blue exclusion assay.

### **Western Blotting**

Sf-21-*PsINP* cells were washed with 1X PBS and aspirated. Cells were lysed using 100 µl 1X sodium dodecyl sulfate (SDS) sample buffer per sample and transferred to microcentrifuge tubes, containing  $1 \cdot 10^6$ ,  $2.5 \cdot 10^6$ , and  $4.5 \cdot 10^6$  cells. Each cell sample was sonicated for 20 seconds. A 20 µl portion of each sample was then heated to 95 °C for 5 min, and loaded onto an SDS polyacrylamide gel (SDS-PAGE gel). A 10 µl quantity of Precision Plus Protein Dual Color Standard (Bio-Rad, Hercules, CA) was loaded into the first lane of the gel. The gel was allowed to run for 30 min at 200 V, and proteins were transferred to a nitrocellulose membrane, using a 100 V current for 30 min. The membrane was incubated in 25 ml blocking buffer (1X tris-buffered saline (TBS), 0.1% Tween-20, 5% nonfat dry milk) for one hour at room temperature, then subjected to 3 5-minute washes with 15 ml 1X TBS and 0.1% Tween-20 (TBS/T) each. A 1:1000 primary antibody dilution buffer was prepared, comprised of 1X TBS/T, 5% BSA, and 10 µl primary His-tag rabbit antibody (Cell Signaling Technology, Danvers, MA), and the membrane was incubated in this solution on a rocking platform at 4 °C overnight ( $\geq 16$  h). Following this incubation, the membrane was washed with 15 ml TBS/T for 5 min, 3 times. A 1:2000 secondary antibody solution, consisting of 10 ml blocking buffer and 5 µl secondary anti-rabbit IgG antibody (Cell Signaling Technology, Danvers, MA), was applied to the membrane, and incubated on a rocking platform at room temperature for one h. After 3 5-minute washes with 15 ml TBS/T, proteins were

visualized using a 4-chloro-1-naphthol/3,3'-diaminobenzidine tetrahydrochloride (CN/DAB) substrate kit (Fisher Scientific, Waltham, MA).

### **Protein modeling**

The nucleotide sequence transfected into Sf-21 cells was submitted for computational modeling to the I-TASSER server (Ambrish et al., 2010; Zhang, 2008).

### **Statistical analysis**

Results were analyzed using Sigma Plot 11 software. Statistical analyses (ANOVA followed by Holm-Šídák comparison and student's t-test) were performed on the results, which are reported as mean  $\pm$  standard error.

## RESULTS

To determine whether intracellular expression of the water-structuring protein *PsINP* reduces cryogenic injury during cell freezing, the impact of buffer A on cell viability before the onset of freezing was evaluated. Because transgenic and control cells are exposed to buffer A—which is hyperosmotic and mimics the intracellular ion composition—during freezing, cell membrane integrity was assessed in Sf-21-WT and Sf-21-*PsINP* cells suspended in buffer A for up to 4 h. Cell membrane integrity declined in a time-dependent manner for Sf-21 and transgenic *PsINP*-expressing cells (Sf-21-*PsINP*) incubated at 27 °C. Viability of the two different cell types differed significantly at 1 h and 2 h ( $n = 6$ ,  $p < 0.050$ ). After 4 h, the proportion of Sf-21-WT cells retaining membrane integrity was 0.42, and for Sf-21-*PsINP* cells, this proportion was 0.43. With the exception of Sf-21-WT at  $t(1)$ , all values for membrane integrity significantly differed from  $t(0)$  (Fig. 2).

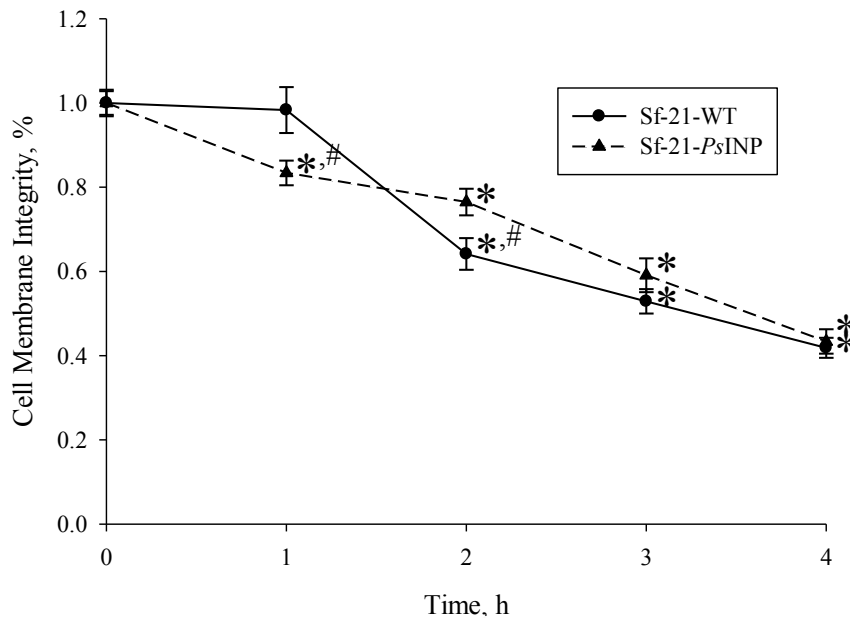


**Figure 2.** Proportions of cells retaining cell membrane integrity, assessed hourly, for Sf-21-WT and Sf-21-*PsINP* cells incubated in buffer A at 27 °C for 4 h ( $n = 6$ ,  $p > 0.050$ ). \* denotes statistical significance, relative to  $t(0)$ . # denotes statistical significance between cell types at a given time point.

After assessing the effect of hyperosmotic stress exerted by buffer A on the two cells types, a freeze-thaw assay was conducted to investigate the impact of freezing on Sf-21-WT and Sf-21-*Ps*INP cell membrane integrity. A difference in the amount of cells with intact cell membranes was observed between the two cell types following the freeze-thaw assay ( $n = 6, p < 0.050$ ). Sf-21-WT cells retained  $60.06\% \pm 3.25\%$  membrane integrity, while  $71.62\% \pm 3.41\%$  of Sf-21-*Ps*INP cell membranes remained intact (Fig. 3).

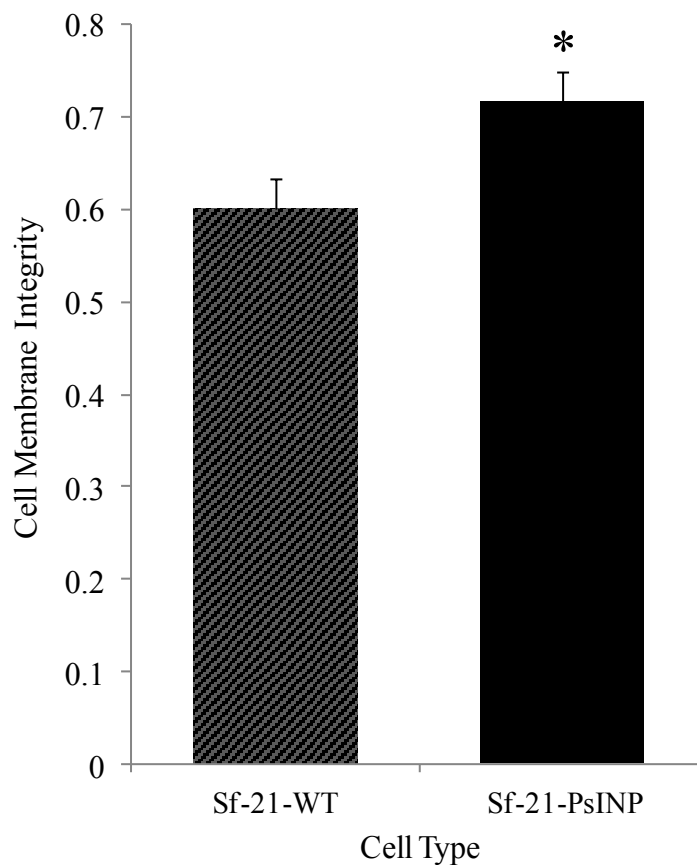


**Figure 3.** Proportions of Sf-21-WT and Sf-21-*Ps*INP cells retaining membrane integrity following one freeze-thaw cycle ( $n = 6, p < 0.050$ ). \* denotes statistical significance.



In order to confirm expression of *PsINP*, Sf-21-*PsINP* cells were characterized using western blotting techniques. Following this procedure, bands were observed at masses of 77 kD, 90 kD, and 97 kD for samples of  $10^6$ ,  $2.5 \cdot 10^6$ , and  $4.5 \cdot 10^6$  cells,

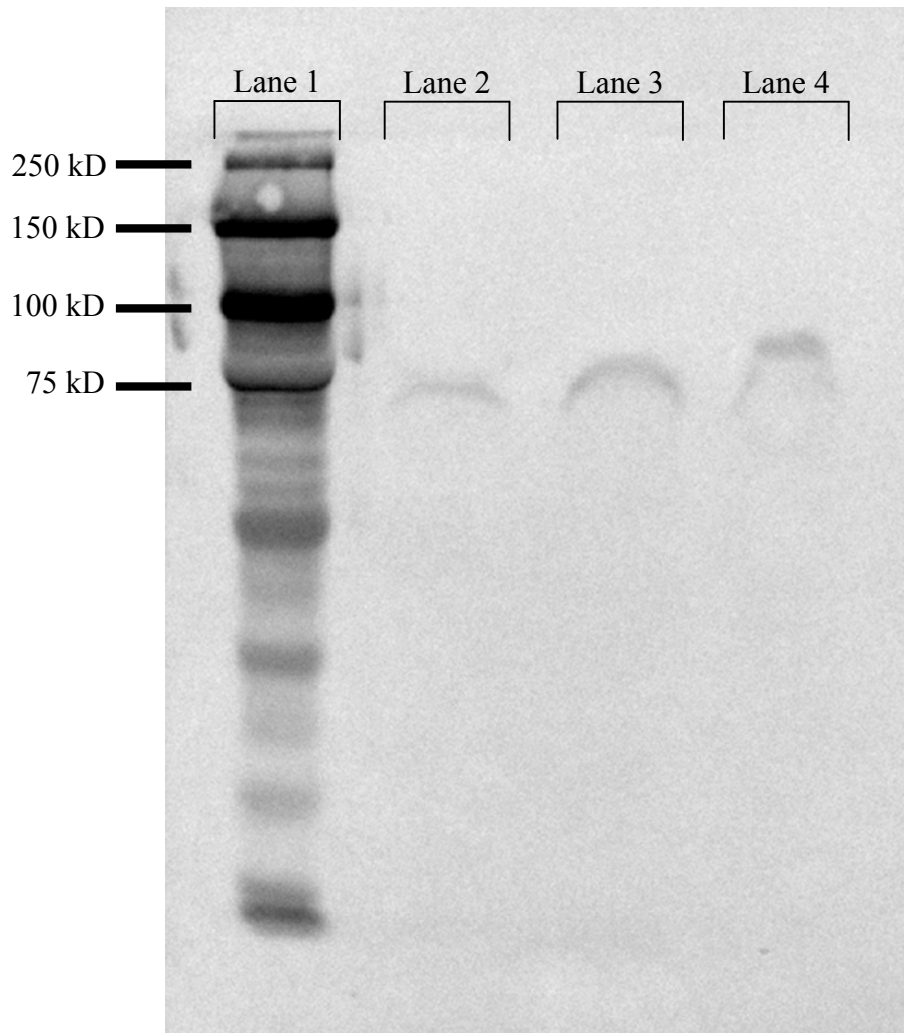


**Figure 4.** Western blot characterization of protein extracted from Sf-21-*PsINP* cells. Lanes, from left to right, contained: Precision Plus Protein Dual Color Standard,  $10^6$ ,  $2.5 \cdot 10^6$ , and  $4.5 \cdot 10^6$  cells respectively (Fig. 4).

To investigate the three dimensional structure of *Ps*INP, an *in silico* approach was taken. The *Ps*INP protein model generated on the I-TASSER server is a  $\beta$ -helical structure with a highly repetitive motive sequence (Fig. 5). A confidence score (C-score) is assigned to each model produced, ranging between -5 and 2; increasing C-score corresponds to increasing model confidence. This score is used to determine a template modeling score (TM-score). TM-scores indicate structural similarity between two protein structures, and usually compare some predicted model to a known native structure. Because the exact structure of *Ps*INP is unknown, an algorithm is used to approximate the TM-score based on known correlations between C-scores and TM-scores. A TM-score  $> 0.5$  indicates a model of correct topology. For the *Ps*INP model, the C-score was -1.60, and the experimental TM-score was 0.52. These values support a high degree of reliability for the generated *Ps*INP model.

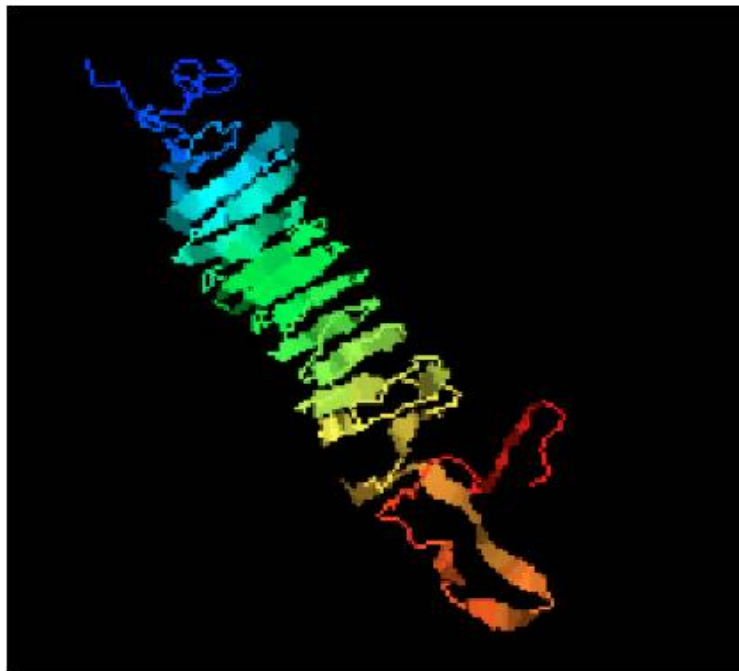


**Figure 5.** Predicted  $\beta$ -helical tertiary structure of *Ps*INP, generated on the I-TASSER server.

## DISCUSSION

The overall goal of this study was to investigate whether the  $\beta$ -helical, water-structuring protein *PsINP* can increase the viability of *PsINP*-expressing cells following a freeze-thaw cycle. A direct link must be established between *PsINP* expression and an increase in maintained cell membrane integrity for this hypothesis to be supported. Therefore, it is important to ensure that the intracellular presence of *PsINP* is the only variable contributing to proportions of viable cells observed after freezing and thawing.

The cell incubation assay examined the impact of buffer A—a hyperosmotic environment ( $\sim 430$  mOsM)—on cell membrane integrity, and whether this impact was dependent upon the cell type. Cell membrane integrity was maintained in lower proportions in Sf-21-*PsINP* cells at 1 h, establishing that *PsINP* expression does not positively affect cellular responses to the freezing medium prior to ice-nucleation. Therefore, any difference between Sf-21-WT and Sf-21-*PsINP* cells in retained membrane integrity following a freeze-thaw cycle can be attributed to the expression of *PsINP*. It should be noted that Sf-21-*PsINP* cells are negatively impacted by a hyperosmotic environment for the first 1 h, relative to Sf-21-WT cells. This difference may be driven by the function of *PsINP* as a water-structuring protein; free water molecules within the cell are expected to be bound by *PsINP* to a minimal degree at temperatures above the ice nucleation temperature. This effect may exaggerate the impact of hyperosmotic extracellular conditions.

These data also provide an estimate of how much the cell membrane integrity might decline before the samples completely freeze. Prior to freezing, samples were suspended in buffer A at room temperature ( $\sim 21$  °C) and then cooled to  $-80$  °C at a rate of

$-1\text{ }^{\circ}\text{C} \cdot \text{min}^{-1}$ . The 1.0 ml samples will therefore be completely frozen within one hour, and at this time point, at least  $\sim 85\%$  of cell membranes remains intact (the lower value at 1 h was  $84.95 \pm 3.64\%$  for Sf-21-*Ps*INP cells). For *Ps*INP cells at 1 h, this decrease of  $\sim 15\%$  should be considered a maximum projection for cell membrane integrity following a freeze-thaw cycle. As 28.38% of Sf-21-*Ps*INP cells actually lost membrane integrity following complete freezing and thawing,  $\sim 50\%$  of this loss is due to hyperosmotic stress and corresponds to the observed  $\sim 15\%$  loss following the incubation assay. The remaining  $\sim 50\%$  loss is the result of cryoinjury.

The expression of *Ps*INP increases the proportion of cells with intact membranes. This may be due to the repetitive TXT motif, common to all INPs, found within *Ps*INP. In order to determine the exact role these repeats play in conferring cryoprotection to Sf-21-*Ps*INP cells, an additional line of Sf-21 cells could be developed which expresses variant forms of the *Ps*INP gene. Graether et al. (2000) carried out a similar study, examining the function of the TXT motif in a spruce budworm AFP by replacing specific threonine residues with leucine. Substituting leucine molecules (a hydrophobic amino acid) for threonine residues (with a polar neutral side chain) within TXT repeats would allow the proposed influence of threonyl oxygens on the ice nucleation activity of the total protein to be quantified. Cells expressing this modified form of *Ps*INP would be expected to maintain lower proportions of cell membrane integrity. Additionally, solutions of *Ps*INP, and its altered counterpart dissolved in buffer A, should have different freezing points, with *Ps*INP increasing the freezing point of the solution more effectively than the leucine containing protein.

The predicted molecular weight of *Ps*INP is 26.99 kD, much smaller than the observed Western Blot bands. However, other INPs produced by *P. syringae* are known to aggregate during processing for Western Blotting (Ruggles et al., 1993). The greater the size of an ice nucleator, the higher the nucleation temperature. This effect becomes exaggerated at increasing temperatures; as the nucleation temperature approaches 0 °C, greater nucleator mass is required to affect diminishing increases in nucleation temperature (Burke and Lindow, 1990). The tendency of INPs to form aggregates capable of inciting ice nucleation at elevated temperatures may explain the protein bands with higher than anticipated masses.

The computational model of *Ps*INP is consistent with other models of INPs and AFPs as  $\beta$ -helical structures (Graether et al., 2000; Liou et al., 2000; Graether and Jia, 2001; Garnham et al., 2011). The reliability of the predicted structure supports the hypothesis that  $\beta$ -sheets within the protein serve as planar surfaces at which water molecules may interact with threonyl oxygens and initiate homogeneous nucleation.

## CONCLUSIONS

The major conclusions of this study are summarized as follows:

- (1) Expression of the protein *PsINP* provided no advantage to cells exposed to a hyperosmotic and intracellular-like environment; in fact, Sf-21-*PsINP* cells were negatively impacted by these conditions (relative to Sf-21-WT cells) for the first 2 h of incubation.
- (2) Sf-21-*PsINP* cells maintained cell membrane integrity in greater proportions than Sf-21-WT cells, and this difference can be directly attributed to *PsINP* expression.
- (3) Western Blot characterization confirms the transgenic expression of *PsINP* and also illustrates the tendency of INPs to aggregate.
- (4) The computational model generated on the I-TASSER server is consistent with other published models of INPs and AFPs, and with the hypothesis that threonyl residues located in  $\beta$ -sheet regions mediate the initiation of ice nucleation.

## LITERATURE CITED

- Ambrish, R., Kucukural, A. and Zhang, Y. 2010. I-TASSER: a unified platform for automated protein structure and function prediction. *Nature Protocols*. 5: 725-738.
- Battan, L. J. 1969. Harvesting the clouds. Advances in weather modification. Doubleday & Co., Inc., Garden City, New York.
- Burke, M. J. and Lindow, S. E. 1990. Surface properties and size of the ice nucleation site in ice nucleation active bacteria: theoretical considerations. *Cryobiology*. 27: 80-84.
- DeVries, A. L. and Wohlschlag, D. E. 1969. Freezing resistance in some Antarctic fishes. *Science*. 163: 1073-1075.
- Dumont, F., Marechal, P. and Gervais, P. 2004. Cell size and water permeability as determining factors for cell viability after freezing at different cooling rates. *Applied and Environmental Microbiology*. 70: 268-272.
- Fei, Y. B., Cao, P. X., Gao, S. Q., Wang, B., Wei, L. B., Zhao, J., Chen, G. and Wang, B. H. 2008. Purification and structure analysis of antifreeze proteins from *Ammopiptanthus mongolicus*. *Preparative Biochemistry and Biotechnology*. 38: 179-190.
- Garnham, C. P., Campbell, R. L., Walker, V. K. and Davies, P. L. 2011. Novel dimeric  $\beta$ -helical model of an ice nucleation protein with bridged active sites. *BMC Structural Biology*. 11: 36.

- Gilbert, J. A., Hill, P. J., Dodd, C. E. R. and Laybourn-Parry, J. 2004. Demonstration of antifreeze protein activity in Antarctic lake bacteria. *Microbiology*. 150: 171-180.
- Govindarajan, A. G. and Lindow, S. E. 1988. Phospholipid requirement for expression of ice nuclei in *Pseudomonas syringae* and *in vitro*. *Journal of Biological Chemistry*. 263: 9333-9338.
- Govindarajan, A. G. and Lindow, S. E. 1988. Size of bacterial ice-nucleation sites measured *in situ* by radiation inactivation analysis. *Proceedings of the National Academy of Sciences of the United States of America*. 85: 1334-1338.
- Graether, S. P. and Jia, Z. 2001. Modeling *Pseudomonas syringae* ice-nucleation protein as a  $\beta$ -helical protein. *Biophysical Journal*. 80: 1169-1173.
- Graether, S. P., Kuiper, M. J., Gagné, S. M., Walker, V. K., Jia, Z., Sykes, B. D. and Davies, P. L. 2000. B-helix structure and ice-binding properties of a hyperactive antifreeze protein from an insect. *Nature*. 406: 325-328.
- Gurian-Sherman, D. and Lindow, S. E. 1993. Bacterial ice nucleation: significance and molecular basis. *FASEB Journal*. 7: 1338-1343.
- Hawes, T. C., Marshall, C. J. and Wharton, D. A. 2011. Antifreeze proteins in the Antarctic springtail, *Gressittacantha terranova*. *Journal of Comparative Physiology B*. 181: 713-719.
- Hoshino, T., Kiriaki, M., Ohgiya, S., Fujiwara, M., Kondo, H., Nishimiya, Y., Yumoto, I. and Tsuda, S. 2003. Antifreeze proteins from snow mold fungi. *Canadian Journal of Botany*. 81: 1175-1181.



- Janech, M. G., Krell, A., Mock, T., Kang, J. S. and Raymond, J. A. 2006. Ice-binding proteins from sea ice diatoms (Bacillariophyceae). *Journal of Phycology*. 42: 410-416.
- Li, T., Donadio, D., Russo, G. and Galli, G. 2011. Homogeneous ice nucleation from supercooled water. *Physical Chemistry Chemical Physics*. 13: 19807-19813.
- Lindow, S. E., Army, D. C. and Upper, C. D. 1982. Bacterial ice nucleation: a factor in frost injury to plants. *Journal of Plant Physiology*. 70: 1084-1089.
- Liou, Y., Tocilj, A., Davies, P. L. and Jia, Z. 2000. Mimicry of ice structure by surface hydroxyls and water of a  $\beta$ -helix antifreeze protein. *Nature*. 406: 322-324.
- Maki, L. R., Galyan, E. L., Mei-Mon, C. and Caldwell, D. R. 1974. Ice nucleation induced by *Pseudomonas syringae*. *Applied Microbiology*. 28: 456-459.
- Mazur, P. 1963. Kinetics of water loss from cells at subzero temperatures and the likelihood of intracellular freezing. *Journal of General Physiology*. 47: 347-369.
- Mazur, P. 2010. A biologist's view of the relevance of thermodynamics and physical chemistry to cryobiology. *Cryobiology*. 60: 4-10.
- Mazur, P., Shinsuke, S., Pinn, I. L., Kleinhans, F. W. and Edashige, K. 2005. Extra- and intracellular ice formation in mouse oocytes. *Cryobiology*. 51: 29-53.
- Missous, G., Thammavongs, B., Dieuleveux, V., Gueguen, M. and Panff, J. M. 2007. Improvement of the cryopreservation of the fungal starter *Geotrichum candidum* by artificial nucleation and temperature downshift control. *Cryobiology*. 55: 66-71.

- Morris, C. E., Georgakopoulos, D. G. and Sands, D. C. 2004. Ice nucleation active bacteria and their potential role in precipitation. *Journal de Physique*. 121: 87-103.
- Morris, C. E., Kinkel, L. L., Kun, X., Prior, P. and Sands, D. C. 2007. A surprising niche for the plant pathogen *Pseudomonas syringae*. *Infection, Genetics and Evolution*. 7: 84-92.
- Morris, C. E., Sands, D. C., Vanneste, J. L., Montarry, J., Oakley, B., Guilbaud, C. and Glaux, C. 2010. Inferring the evolutionary history of the plant pathogen *Pseudomonas syringae* from its biogeography in headwaters of rivers in North America, Europe, and New Zealand. *American Society for Microbiology*.
- Morris, C. E., Sands, D. C., Vinatzer, B. A., Glaux, C., Guilbaud, C., Buffière, A., Yan, S., Cominguea, H. and Thompson, B. M. 2008. The life history of the plant pathogen *Pseudomonas syringae* is linked to the water cycle. *Journal of the International Society for Microbial Ecology*. 2: 321-334.
- Mueller, G. M., Wolber, P. K. and Warren, G. J. 1990. Clustering of ice nucleation protein correlates with ice nucleation activity. *Cryobiology*. 27: 416-422.
- Ruggles, J. A., Nemecek-Marshall, M. and Fall, R. 1993. Kinetics of appearance and disappearance of classes of bacterial ice nuclei support an aggregation model for ice nucleus assembly. *Journal of Bacteriology*. 175: 7216-7221.
- Toner, M., Cravalho, E. G., Stachecki, J., Fitzgerald, T., Tompkins, R. G., Yarmush, M. L. and Armant, D. R. 1993. Nonequilibrium freezing of one-cell mouse embryos: membrane integrity and developmental potential. *Biophysical Journal*. 64: 1908-1921.

- Walker, V. K., Palmer, G. R. and Voordouw, G. 2006. Freeze-thaw tolerance and clues to the winter survival of a soil community. *Applied and Environmental Microbiology*. 72: 1784-1792.
- Wolber, P. K., Deininger, C.A., Southworth, M.W., Vandekerckhove, J., van Mantagu, M. and Warren, G. J. 1986. Identification and purification of a bacterial ice-nucleation protein. *Proceedings of the National Academy of Sciences of the United States of America*. 83: 7256-7260.
- Zhang, Y. 2008. I-TASSER: server for protein 3D structure prediction. *BMC Bioinformatics*. 9: 40.